HHS Public Access

Author manuscript

N Engl J Med. Author manuscript; available in PMC 2024 August 21.

Published in final edited form as:

N Engl J Med. 2024 June 13; 390(22): 2047–2060. doi:10.1056/NEJMoa2401361.

Risk of second malignancies and T-cell lymphoma after chimeric antigen receptor T-cell therapy

Mark P. Hamilton, M.D., Ph.D.[1,2,3], **Takeshi Sugio, M.D., Ph.D.**[1,4], **Troy Noordenbos, M.D., Ph.D.**[1,4], **Shuyu Shi, B.Med.**[5], **Philip L. Bulterys, M.D., Ph.D.**[6], **Chih Long Liu, Ph.D.**[1,4], **Xiaoman Kang, B.S.**[1,4], **Mari N. Olsen, B.S.**[1,4], **Zinaida Good, Ph.D.**[2,7], **Saurabh Dahiya, M.D., F.A.C.P.**[2,3], **Matthew J. Frank, M.D., Ph.D.**[2,3], **Bita Sahaf, Ph.D.**[2], **Crystal L. Mackall, M.D.**[2,4,8], **Dita Gratzinger, M.D., Ph.D.**[6], **Maximilian Diehn, M.D., Ph.D.**[4,9,10], **Ash A. Alizadeh, M.D., Ph.D.**[1,4,10], **David B. Miklos, M.D., Ph.D.**[2,3,4]

[1]Division of Oncology, Department of Medicine, Stanford University School of Medicine, Stanford, CA 94305, USA.

[2]Center for Cancer Cell Therapy, Stanford Cancer Institute, Stanford University School of Medicine, Stanford, CA 94305, USA.

[3]Division of Blood and Marrow Transplantation and Cellular Therapy, Department of Medicine, Stanford University School of Medicine, Stanford, CA 94305, USA.

[4]Stanford Cancer Institute, Stanford University, Stanford, CA, 94305, USA

[5]Department of Bioengineering, Stanford University Schools of Medicine and Engineering, Stanford, CA94305, USA.

[6]Department of Pathology, Stanford University School of Medicine, Stanford, CA 94305, USA.

[7]Department of Biomedical Data Science, Stanford University School of Medicine, Stanford, CA, 94305, USA

[8]Division of Hematology/Oncology, Department of Pediatrics, Stanford University School of Medicine, Stanford, CA, 94305, USA

[9]Department of Radiation Oncology, Stanford University School of Medicine, Stanford, CA 94305, USA.

[10]Institute for Stem Cell Biology and Regenerative Medicine, Stanford University, Stanford, CA, 94305, USA

Abstract

Background—Secondary cancer risk after CAR T-cell therapy is an emerging concern, especially T-cell neoplasms related to viral vector integration.

Corresponding Author: Dr. Ash A. Alizadeh, arasha@stanford.edu.
Dr. Hamilton, Dr. Sugio, and Dr. Noordenbos contributed equally to this article.
Dr. Alizadeh and Dr. Miklos contributed equally to this article.

Disclosure forms provided by the authors are available with the full text of this article at NEJM.org.

Methods—The clinical experience with adoptive cellular CAR therapy at Stanford since 2016 was reviewed and the occurrence of second malignancies ascertained. In one case of secondary T-cell lymphoma, a broad array of molecular, genetic, and cellular techniques were used to interrogate the tumor, the CAR-T cells, and the normal hematopoietic cells in the patient.

Results—We describe the second cancer risk in 724 patients receiving T-cell therapies at our center. We identified a lethal T-cell lymphoma after axicabtagene ciloleucel therapy for DLBCL, and deeply profiled both tumors. Each lymphoma had molecularly distinct immunophenotypes and genomic profiles, but both were EBV+ and associated with DNMT3A and TET2 mutant clonal hematopoiesis. We found no evidence of oncogenic retroviral integration using multiple techniques.

Conclusion—These results highlight the rarity of secondary neoplasms, while providing a framework for defining clonal relationships and viral vector monitoring.

(Funded by NCI and others.)

Introduction:

Despite the remarkable therapeutic efficacy of commercial chimeric antigen receptor (CAR) T-cell therapies,[1-9] concerns over toxicities remain. Recent reports described cases of post-infusion T-cell lymphoma (TCL) after CAR therapy, which can be associated with integration of the CAR T-cell vector into the malignant lymphocytes[10-15]. These reports mirror prior concerns over vector integration causing direct tumorigenesis after gene therapy[16-18].

The concern over vector integration leading to T-cell leukemia/lymphoma (TCL) was highlighted by a recent Food and Drug Administration (FDA) announcement focused on gathering evidence of additional post-CAR TCLs after commercial CAR T-cell therapy, while also noting that benefits of these therapies likely substantially outweigh potential risks[11]. Since this FDA alert describing 22 TCL cases with 3 interrogated for viral vectors, another $CD8^+$ TCL was reported harboring a *JAK3* lesion and diagnosed ~3 months after commercial CAR19 therapy[10]. The TCL clone was identified at low levels in the blood before CAR19 therapy, and vector levels in the clonal tissue were low. Accordingly, given the relatively small number of reported cases thus far, additional comprehensive genetic characterization of post-CAR TCLs remains essential to understanding the risk of potential post-CAR malignancies, as well as defining the role of vector integration in malignant transformation.

Here we report a single case of an Epstein-Barr virus positive (EBV^+) TCL diagnosed 54 days after CAR therapy, when studying second malignancy incidence among 724 patients infused with adoptive cellular therapies at our institution. We describe the molecular profile of this TCL and the antecedent diffuse large B-cell lymphoma (DLBCL), through deep molecular profiling of both tumors, including by flow cytometric immunophenotyping, targeted and whole exome sequencing, as well as single cell RNA (scRNA) and DNA (scDNA) sequencing of the incident TCL. We also describe the longitudinal blood profiling of cell free DNA (cfDNA) for noninvasive genotyping of each tumor and for monitoring

viral vectors, along with minimal residual disease (MRD) DNA monitoring of B- and T-cell receptor clonotypes.

Methods:

Detailed methods for all molecular techniques are available in the Supplementary Methods section. Methods are additionally detailed in prior studies[19-22].

Case Report

Rarity of Secondary Cancers—We analyzed 791 cell therapy infusions (96.6% CAR T cells, 0.8% cytokine induced killer T cells, 1.5% cytotoxic T lymphocytes, 1.1% specific peptide enhanced affinity receptor T cells, hereafter referred to as CAR T-cell therapy) administered to 724 unique patients at Stanford University Medical Center between 2/4/2016 and 1/15/2024 (Fig 1A, Table S1). After a median follow-up of 15 months, we identified 25 second primary malignancies (SPM) excluding non-melanoma skin cancers. Of 14 hematologic SPMs 13 were myelodysplastic syndrome or acute myeloid leukemia, and 1 was TCL. Eleven SPMs were solid tumors (4 melanomas, 2 prostate carcinomas, 2 breast ductal carcinomas, 1 endometrial adenocarcinoma, 1 lung adenocarcinoma, and 1 metastatic mesothelioma, Fig S1A-B, Table S2). The cumulative incidence of hematologic SPM at 3 years was 6.5% reflecting the rarity of post-CAR SPM as previously reported[15,23,24].

A rare post-CAR19 TCL case

This index TCL arose in a 59-year-old female who received CAR19 therapy for a Stage IV EBV^+ DLBCL, originally presenting in the lymph nodes (LN) and bone marrow (BM). Of note, the patient had a history of psoriasis and eosinophilic fasciitis treated with multiple agents over three years before developing lymphoma (Fig 1B, Fig 2A). After early failures of primary frontline DLBCL induction and second line chemoimmunotherapy regimens, the patient received axicabtagene ciloleucel (axi-cel) CAR19 therapy. Despite achieving a partial metabolic response on day 28 (D+28), the patient subsequently developed significant pancytopenia. On D+54, BM biopsy revealed hemophagocytic lymphohistiocytosis (HLH) associated with a $CD3^+CD4^+EBV^+$ T-cell lymphoma, with positron emission tomography–computed tomography (PET-CT) confirming widespread nodal and marrow disease burden (Fig 1B, Fig 2B). After substantial decline of her performance status, the patient was unable to receive TCL treatment and succumbed to disease on D+62. Of note, this index patient was among 5 total EBV^+ DLBCL cases in our cohort, with 3 other patients experiencing disease progression by D+90 (2 biopsy proven DLBCL relapses, 1 radiographic tumor progression at original primary anatomic site), and 1 patient remaining in remission after CAR19, despite developing a secondary melanoma.

Results:

To better understand any potential role for CAR19 vector integration in driving the index TCL, we performed comprehensive profiling of longitudinal samples from the patient (Fig 1B, Table S3). Immunohistochemical (IHC) features of the original DLBCL were consistent with an aggressive mature B-cell neoplasm with non-germinal center B phenotype (non-

GCB), expressing CD19, CD20, and EBV Encoded small RNA (EBER) in the atypical large B cells, and without evidence for MYC, BCL2, or BCL6 aberrations by fluorescent in situ hybridization. Importantly, at time of DLBCL diagnosis no obvious morphologically abnormal T-cell population was observed, with T cells being EBER negative (Fig 2A, Supplemental Note 1, Fig S1C). In contrast, the subsequent EBV^+ TCL was found to be $CD3^+CD4^+CD8^-EBER^+$, with no evidence of residual DLBCL by morphological or molecular criteria (Fig 2B).

Minimal Residual Disease (MRD) monitoring of the leukocytes from the peripheral blood (PB) and BM revealed rapid eradication of B-cell lymphoma after axi-cel, when using immunoglobulin high throughput sequencing to track the DLBCL B-cell receptor (BCR) immunoglobulin heavy chain clonotype (Fig 2C). Similarly, using simultaneous tumor and effector cell profiling (STEP) of cell-free DNA with CAPP-Seq[21], we again observed clearance of the prior B-cell lymphoma derived circulating tumor DNA (ctDNA, Fig 2D). We further performed TCR tracing and found that the dominant *TCRB* clonotype of the TCL identified in the day +54 BM sample was also detectable before infusion in the D-88 lymph node and D-50 blood at low levels (0.006% and 0.0005% of cells respectively; Fig 2C). This same *TCRB* clonotype emerged on D+28 in the periphery and then dominating cfDNA by D+54 (Fig 2D). Axi-cel expansion in the peripheral blood measured by flow cytometry (Fig 2E, Fig S2A) demonstrated a normal peak[19] and remained at low levels until D+54. Coincident with development of the TCL clone and HLH, the plasma viral load for EBV also rose dramatically following CAR19 therapy (Fig 2F).

Shared & Distinctive Tumor Molecular Profiles

To better understand the clonal relationships between this TCL relative to the antecedent DLBCL, we performed comprehensive genetic profiling using CAPP-Seq and whole exome sequencing of three pre-infusion tumor samples (T1-3), four longitudinal plasma samples (P1-4), and the TCL itself (T4, Fig 1B, Fig 2G). Gene expression profiles inferred noninvasively from plasma using EPIC-seq[25] demonstrated increased expression of several immune cell and inflammatory markers alongside CD3 and CD4, consistent with origination of the TCL in the background of HLH (Fig 2G panel 1, Fig S2B). Molecular profiling of the DLBCL demonstrated a mutation pattern consistent with prior EBV+ B-cell lymphoma[26,27] that was not detected in the TCL sample (Fig 2G panel 2). Though the aggregate ctDNA MRD level was below the limit of detection, a single *CPEB2* mutation originally present in DLBCL tumors was also detected in D+54 plasma; as such, small amounts of residual DLBCL or its progenitor clone could not be entirely ruled out. Conversely, the index TCL demonstrated a mutational spectrum consistent with mature T-cell neoplasms, including an emergent *FYN* R176C activating mutation that was not present in the original DLBCL (Fig 2G panel 3). Both DLBCL and TCL tumor specimens contained mutations in *TET2* and *DNMT3A* at high variant allelic fractions suggesting derivation from clonal hematopoiesis (Fig 2G panel 4). The DLBCL tumor harbored a chr3q amplification and ch7q deletion which were absent in the TCL, while the TCL harbored a chr1q amplification and chr6q deletion that were not detectable in the DLBCL tumor (Fig 2G panel 5, Fig S2C). Collectively, these data suggest that while the DLBCL and TCL were molecularly distinct,

the presence of and shared lesions including mutations in *TET2* and *DNMT3A* implicate a common progenitor.

Evidence against oncogenic vector expression

To better define the phenotype of this post-CAR19 TCL and assess it for presence of the viral vector, we performed scRNA profiling of the bone marrow in the axi-cel treated patient using single cell RNA sequencing (scRNA-seq), relying on 2 axi-cel products and 5 healthy adults as positive and negative controls for the retroviral vector, respectively (Fig 3A, Fig S3A-B). Within bone marrow cells from the index lesion, we could readily identify a distinctive T-cell cluster representing the malignant T cells (Fig S3C-D). These T cells were highly clonal when considering diversity at TCR loci (Fig S3E) and had a $CD3^{+}CD4^{+}$ and $CD8^{-}$ phenotype, consistent with the immunophenotype determined by histopathology (Fig S3F). The dominant TCRB clone found in these single cells was indeed identical with that found in the plasma cfDNA by STEP, as well as in the TCL tumor by VDJ profiling using clonoSEQ (Fig 2C-D, Fig 3B).

Inferred copy number profiles of the single cells within the malignant clone demonstrated changes consistent with previously discovered structural rearrangements including 6q loss and 1q gain (Fig S3G) and EBV positivity (Fig S3H). The expressed gene program discovered in scRNA sequencing included *BALF3-5*, *LF1-2*, and *BARF0* suggesting an EBV-related lytic expression pattern[28]. A gene expression profile in the tumor along with its mutation pattern and histopathology were most consistent with PTCL-NOS (Fig S3I)[29]. Axi-cel vector transgene mRNA was conspicuously absent from the TCL tumor specimen (Fig 3C), and consistently, flow cytometry profiling of the bone marrow specimen for surface CAR19 protein levels (FMC63) also failed to support vector expression (Fig S2A). Collectively, these data highlight the absence of evidence to directly implicate axi-cel vector activity at the RNA or protein level in this index TCL.

Evidence against oncogenic vector integration

We next considered whether cryptic axi-cel integration into this TCL genome may not lead to axi-cel RNA or protein expression, yet nevertheless serve as an oncogenic event. As a first step to validate our single cell RNA and protein expression profiling results, we began by testing the index TCL for presence of integrated vector DNA sequences by quantitative PCR (qPCR), comparing levels to D+14 circulating leukocytes, when axi-cel was detected as 3.61% of T cells by flow cytometry (Fig S2A). While axi-cel was reliably detected in D+14 control leukocytes as expected, it was not detected in bone marrow cells containing the TCL above the limit of detection of the assay (Fig S4A).

We also considered whether cryptic retroviral integration and associated structural derangements may occur segmentally, leading to fragments of the integrated axi-cel vector that may not be detectable using a single set of primers. To address this possibility, we first tested for evidence of axi-cel integration into the TCL genome using a 112-probe hybrid capture panel[21] consisting of overlapping 120 bp probes directed against the entire axi-cel retroviral vector (Fig S2B). Using this approach and consistent with our previous results, the axi-cel vector was not detectable in the index TCL sample, despite being reliably detected

at D+7 and D+21 in plasma cfDNA as well as D+14 in circulating leukocytes, as expected during CAR19 T-cell expansion (Fig 2E).

To test the presence of axi-cel DNA more definitively in the index lesion at single cell resolution, we next targeted 11 tiled amplicons spanning the length of the integrated axi-cel vector (Fig S4B). Using cytopenic bone marrow aspirates from 7 unrelated patients post-CAR19 (range D+137 – D+1561) as positive controls, we reliably detected low level axi-cel signal in 5 of 7 controls at a frequency as low as 0.2% (range 0.2% - 1.1%, Fig S4C). Amplicon DNA content per cell correlated with paired RNA-sequencing data within the control subjects (Fig S4D). Concurrent cell surface protein analysis using antibody probes demonstrated that >93% of axi-cel positive cells were identified as T cells, thus validating the sensitivity and specificity of the assay (Fig S4E-H, Supplemental Note 2). The presence of axi-cel in non-transformed bone marrow specimens up to four years after axi-cel treatment indicates the need for caution before assigning vector integration as a method of transformation. Indeed, persistence of CAR is expected at low levels for very prolonged periods post infusion[30].

Having established the accuracy of this single cell assay, we similarly characterized bone marrow containing the index TCL using our scDNA panel with a total of 6723 cells assayed. Using multiplexed antibodies to barcode and index each single cell, a population of $CD3^{+}CD4^{+}CD8^{-}$ T cells consistent with the TCL was again identified along with myeloid cell populations (Fig 3G, Fig S4I). Remarkably, the pre-existing heterozygous DNMT3A R882C and the TET2 L1212Vfs clones were present in 97.9% of these T cells (Fig 3**H**). This finding provides strong evidence for the TCL to be both DNMT3A R882C and TET2 L1212Vfs mutant, and thus likely derived from lymphoid clonal hematopoiesis (L-CHIP) present before infusion. The *TET2* clone was further characterized as hemizygous for L1212Vfs, indicating a concurrent loss of heterozygosity event. Indeed, lineage tracing analysis using copy number variation analysis in cells revealed a *TET2* deletion lacking DNMT3A R882C and TET2 L1212Vfs in 31.5% of all cells (Fig 3D, Fig S4E), indicating TET2 loss of heterozygosity to be the founding clonal event. Following this event, the presence of a subset of *TET2* deleted and *DNMT3A* mutant cells indicated DNMT3A R882C mutation to be a subsequent clonal event. Finally, the L1212Vfs mutation was a third clonal event leading to the founder progenitor clone from which the malignant population derived (Fig S4J-K). The existence of the *DNMT3A* and *TET2* clones throughout the lymphoid and myeloid lineages in different proportions suggests the original clone derived from a hematopoietic stem or progenitor cell (TET2 deletion + DNMT3A R882C + TET2 L1212Vfs was found in 35.8% of the myeloid population).

Despite direct identification of the index lesion at single cell resolution, axi-cel amplification across all 11 amplicons was conspicuously absent, thus providing no evidence for fragmented DNA integration of the vector as a mechanism of tumorigenesis (Fig 3F). Collectively, these results demonstrate the clear absence of evidence to directly implicate the viral vector in this TCL, as determined by multiple sensitive molecular assays to interrogate retroviral vector DNA, RNA, and protein at single cell resolution.

Discussion:

Second primary malignancies are now recognized as a risk after CAR19 therapy with recent reports detailing higher reporting odds ratio for myeloid and T cell SPMs[24]. T-cell lymphomas are of particular interest in this setting, due to the risk of CAR vector integration contributing to oncogenesis. This study describes a comprehensive genomic profiling of a TCL arising after commercial CAR19 at single cell resolution. The methods employed here serve as a resource and a benchmark for characterization of post-CAR malignancies and for vector monitoring. After surveilling for SPM across 724 patients who received cellular therapy at our center, we found TCL to be rare, only accounting for a single case. No evidence was found to implicate direct contribution from the engineered retroviral vector in the index TCL at the DNA, mRNA, or protein level, and when interrogating circulating, tissue resident, and cell-free anatomical compartments. We found this index TCL to be molecularly distinct from the original DLBCL, without evidence for lineage-switch or trans-differentiation. Instead, the TCL clone was first detected before infusion of CAR T-cell therapy at D-88 and was associated with EBV^+ lymphoproliferation, novel structural rearrangement, and a *FYN* activating gene mutation. The pre-existing clonal population retrospectively detected at D-88 in the LN was determined by TCRB detection at a low level (0.006% of cells). While we are unable to definitively establish whether this clone reflects a pre-malignant population or a mature, fully evolved neoplasm, the presence of this clone at detectable levels before infusion supports an underlying susceptibility preceding CAR treatment.

A bidirectional risk between B-cell lymphoma (BCL) and TCL[31] is known where the standardized incidence of TCL after BCL was described at approximately five-fold higher than the general population. This increased incidence was highest in the first year post diagnosis, possibly accounting for reports of TCLs arising within two years of CAR treatment[11]. In this prior report 354 TCLs were observed following 288,478 BCLs (0.12%). Our observation of 1 TCL in 587 BCLs (0.17%, Table S1) is in line with these observations, but the analysis would benefit substantially from a pooled multi-institutional analysis with confirmatory molecular testing for CAR vector insertion.

Supporting *a priori* susceptibility to TCL transformation, the presence of a pre-existing heterozygous DNMT3A R882C and hemizygous TET2 L1212Vfs co-mutant clones in this patient suggests that underlying L-CHIP was likely a modifying factor in this malignancy, even if alone insufficient to drive the T-cell neoplasm. Given the proclivity of EBV to rarely infect hematopoietic stem and progenitor cells leading to chronic-active EBV[32] combined with this patient's known history of a prior EBV^+ B-cell malignancy and underlying multilineage DNMT3A and TET2 mutations, we postulate that this tumor was derived from a DNMT3A and TET2 comutant lymphoid progenitor (Fig 3G). This study highlights the critical potential of L-CHIP mutations to transform into lymphoid malignancies as previously reported[33], and further suggests pre-existing susceptibility to TCL[31]. Such underlying TET2 and DNMT3A mutations are known to drive both EBV^+ DLBCL[27] and EBV^+ TCL[34], thus implicating a common lymphoid progenitor in the formation of both tumors. Given the prevalence of clonal hematopoiesis, screening all pre-CAR patients for such mutations may be infeasible, especially since the likelihood of curing

aggressive lymphoma could outweigh the rare risk of transformation of pre-existing clonal hematopoiesis mutations. In such patients, an alternative pre-emptive strategy to intercept SPMs after CAR T-cell therapies could involve more active noninvasive surveillance for both the dynamics of CAR T cells and clonal hematopoiesis clones under selection, by monitoring of cell-free DNA as described here. Caution is likely warranted if underlying susceptibility mutations are present while treating non-malignant conditions such as autoimmune disease with CAR T cells, especially when other drivers of lymphoproliferation such as EBV are also present.

The tendency of TET2 or DNMT3A deficiency (but not both) to confer selective fitness advantage for engineered T cells is well-known, especially in the CD8 lineage[35]. Nevertheless, despite the prevalence of the circulating CHIP clone harboring lesions in both genes in this patient's blood before leukapheresis, the emergent $CD4^+$ T-cell neoplasm was devoid of vector integration. This surprising observation may perhaps reflect the CD4 versus CD8 lineage-specific constraints for lymphoid clonal hematopoiesis, and/or gene-specific effects[36].

Here we found no evidence for axi-cel incorporation into this tumor by multiple techniques. Our results are in contrast with rare prior reports using other therapeutic vectors including transposons[13,14]. These findings do agree with a recent report of another post-CAR TCL that similarly did not demonstrate CAR19 integration[10]. Importantly, the immunosuppression associated with lymphodepleting chemotherapy, CAR-mediated inflammation, and B-cell aplasia may each have contributed to the EBV-driven lymphoproliferation for the case described here. Additional reports of EBV-driven TCL after CAR therapies would support this hypothesis. This type of immunosuppression is a key long-term toxicity associated with CAR19 therapy[37-39] and underlies non-relapse mortality due to infection. Nevertheless, in our cohort 4 additional patients with EBV^+ DLBCL did not develop subsequent lymphoproliferative disorders, and limited prior reports have suggested that CAR19 therapy can be safe in EBV^+ DLBCL[40].

In summary, this analysis of 724 patients extends prior observations[10] to further suggest that development of TCL CAR T-cell therapy is quite rare and may occur through various mechanisms in susceptible patients. In our index case, despite comprehensive genetic profiling, we could not find evidence for CAR vector integration into the TCL, or evidence for CAR expression. Of note, given the known increased baseline risk of secondary T-cell malignancies in patients with prior B-cell lymphomas even in the absence of CAR therapies[31], when considering a sufficiently large population of patients, the observed T-cell neoplasms after CAR therapies may reflect a bystander instead of a direct effect. In this context, emerging data suggest that an inflammatory memory characterizes a special subset of hematopoietic stem cells that expands with age and is enriched for somatic mutations associated with clonal hematopoiesis[41]. While this remains to be definitively determined, we speculate that such mutant progenitors could be especially prone to CAR associated inflammation and corresponding selection pressures.

Supplementary Material

Refer to Web version on PubMed Central for supplementary material.

Acknowledgements:

We appreciate the contribution of the Mission Bio support team for single cell data analysis as well as the Adaptive Biotechnologies team for their help in tumor receptor tracing. Graphic cartoon objects made in BioRender. Finally, we appreciate the hard work of the Stanford Correlative Science Unit including Zachary Ehlinger, Moksha Desai, Juancarlos Cancilla, and Shriya Syall.

Funding:

Mark P. Hamilton and Takeshi Sugio are fellows of the Leukemia and Lymphoma Society. Troy Noordenbos is supported by a fellowship from the Lymph&Co Foundation. Ash A Alizadeh is a Scholar of the Leukemia & Lymphoma Society and is the Moghadam Family Professor of Medicine at Stanford University. This work was supported by NCI R01CA233975, NCI P01 CA049605, the Virginia and D.K. Ludwig Fund for Cancer Research, Kite-Gilead, and Adaptive Biotechnologies. The content is solely the responsibility of the authors and does not necessarily represent the official views of the US National Institutes of Health.

References:

1. Neelapu SS, Locke FL, Bartlett NL, et al. Axicabtagene Ciloleucel CAR T-Cell Therapy in Refractory Large B-Cell Lymphoma. The New England journal of medicine 2017;377(26):2531–2544. DOI: 10.1056/NEJMoa1707447. [PubMed: 29226797]
2. Locke FL, Miklos DB, Jacobson CA, et al. Axicabtagene Ciloleucel as Second-Line Therapy for Large B-Cell Lymphoma. The New England journal of medicine 2022;386(7):640–654. DOI: 10.1056/NEJMoa2116133. [PubMed: 34891224]
3. Schuster SJ, Bishop MR, Tam CS, et al. Tisagenlecleucel in Adult Relapsed or Refractory Diffuse Large B-Cell Lymphoma. The New England journal of medicine 2019;380(1):45–56. DOI: 10.1056/NEJMoa1804980. [PubMed: 30501490]
4. Bishop MR, Dickinson M, Purtill D, et al. Second-Line Tisagenlecleucel or Standard Care in Aggressive B-Cell Lymphoma. The New England journal of medicine 2022;386(7):629–639. DOI: 10.1056/NEJMoa2116596. [PubMed: 34904798]
5. Abramson JS, Palomba ML, Gordon LI, et al. Lisocabtagene maraleucel for patients with relapsed or refractory large B-cell lymphomas (TRANSCEND NHL 001): a multicentre seamless design study. The Lancet 2020;396(10254):839–852. DOI: 10.1016/s0140-6736(20)31366-0.
6. Kamdar M, Solomon SR, Arnason J, et al. Lisocabtagene maraleucel versus standard of care with salvage chemotherapy followed by autologous stem cell transplantation as second-line treatment in patients with relapsed or refractory large B-cell lymphoma (TRANSFORM): results from an interim analysis of an open-label, randomised, phase 3 trial. Lancet 2022;399(10343):2294–2308. DOI: 10.1016/S0140-6736(22)00662-6. [PubMed: 35717989]
7. Berdeja JG, Madduri D, Usmani SZ, et al. Ciltacabtagene autoleucel, a B-cell maturation antigen-directed chimeric antigen receptor T-cell therapy in patients with relapsed or refractory multiple myeloma (CARTITUDE-1): a phase 1b/2 open-label study. Lancet 2021;398(10297):314–324. (In eng). DOI: 10.1016/s0140-6736(21)00933-8. [PubMed: 34175021]
8. Rodriguez-Otero P, Ailawadhi S, Arnulf B, et al. Ide-cel or Standard Regimens in Relapsed and Refractory Multiple Myeloma. New England Journal of Medicine 2023;388(11):1002–1014. DOI: 10.1056/NEJMoa2213614. [PubMed: 36762851]
9. Munshi NC, Anderson LD, Shah N, et al. Idecabtagene Vicleucel in Relapsed and Refractory Multiple Myeloma. New England Journal of Medicine 2021;384(8):705–716. DOI: 10.1056/NEJMoa2024850. [PubMed: 33626253]
10. Ghilardi G, Fraietta JA, Gerson JN, et al. T-cell Lymphoma and Secondary Primary Malignancy Risk After Commercial CAR T-cell Therapy. Nature medicine 2024. DOI: 10.1038/s41591-024-02826-w.

11. Verdun N, Marks P. Secondary Cancers after Chimeric Antigen Receptor T-Cell Therapy. New England Journal of Medicine 2024. DOI: 10.1056/NEJMp2400209.
12. Levine BL, Pasquini MC, Connolly JE, et al. Unanswered questions following reports of secondary malignancies after CAR-T cell therapy. Nature medicine 2024. DOI: 10.1038/s41591-023-02767-w.
13. Harrison SJ, Nguyen T, Rahman M, et al. CAR+ T-Cell Lymphoma Post Ciltacabtagene Autoleucel Therapy for Relapsed Refractory Multiple Myeloma. Blood 2023;142:6939. DOI: 10.1182/blood-2023-178806.
14. Bishop DC, Clancy LE, Simms R, et al. Development of CAR T-cell lymphoma in 2 of 10 patients effectively treated with piggyBac-modified CD19 CAR T cells. Blood 2021;138(16):1504–1509. DOI: 10.1182/blood.2021010813. [PubMed: 34010392]
15. Steffin DHM, Muhsen IN, Hill LC, et al. Long-term follow-up for the development of subsequent malignancies in patients treated with genetically modified IECs. Blood 2022;140(1):16–24. DOI: 10.1182/blood.2022015728. [PubMed: 35325065]
16. Hacein-Bey-Abina S, Von Kalle C, Schmidt M, et al. LMO2-associated clonal T cell proliferation in two patients after gene therapy for SCID-X1. Science 2003;302(5644):415–9. (In eng). DOI: 10.1126/science.1088547. [PubMed: 14564000]
17. Hacein-Bey-Abina S, von Kalle C, Schmidt M, et al. A serious adverse event after successful gene therapy for X-linked severe combined immunodeficiency. The New England journal of medicine 2003;348(3):255–6. (In eng). DOI: 10.1056/nejm200301163480314. [PubMed: 12529469]
18. Hacein-Bey-Abina S, Garrigue A, Wang GP, et al. Insertional oncogenesis in 4 patients after retrovirus-mediated gene therapy of SCID-X1. The Journal of clinical investigation 2008;118(9):3132–42. (In eng). DOI: 10.1172/jci35700. [PubMed: 18688285]
19. Hamilton MP, Craig E, Gentille Sanchez C, et al. CAR19 monitoring by peripheral blood immunophenotyping reveals histology-specific expansion and toxicity. Blood Advances 2024. DOI: 10.1182/bloodadvances.2024012637.
20. Good Z, Spiegel JY, Sahaf B, et al. Post-infusion CAR TReg cells identify patients resistant to CD19-CAR therapy. Nature medicine 2022;28(9):1860–1871. DOI: 10.1038/s41591-022-01960-7.
21. Sworder BJ, Kurtz DM, Alig SK, et al. Determinants of resistance to engineered T cell therapies targeting CD19 in large B cell lymphomas. Cancer cell 2022. DOI: 10.1016/j.ccell.2022.12.005.
22. Alig SK, Shahrokh Esfahani M, Garofalo A, et al. Distinct Hodgkin lymphoma subtypes defined by noninvasive genomic profiling. Nature 2024;625(7996):778–787. DOI: 10.1038/s41586-023-06903-x. [PubMed: 38081297]
23. Hsieh EM, Myers RM, Yates B, et al. Low rate of subsequent malignant neoplasms after CD19 CAR T-cell therapy. Blood Adv 2022;6(17):5222–5226. (In eng). DOI: 10.1182/bloodadvances.2022008093. [PubMed: 35834728]
24. Elsallab M, Ellithi M, Lunning MA, et al. Second Primary Malignancies After Commercial CAR T Cell Therapy: Analysis of FDA Adverse Events Reporting System (FAERS). Blood 2024. DOI: 10.1182/blood.2024024166.
25. Esfahani MS, Hamilton EG, Mehrmohamadi M, et al. Inferring gene expression from cell-free DNA fragmentation profiles. Nature biotechnology 2022;40(4):585–597. DOI: 10.1038/s41587-022-01222-4.
26. Frontzek F, Staiger AM, Wullenkord R, et al. Molecular profiling of EBV associated diffuse large B-cell lymphoma. Leukemia : official journal of the Leukemia Society of America, Leukemia Research Fund, UK 2023;37(3):670–679. (In eng). DOI: 10.1038/s41375-022-01804-w.
27. Li Y, Xu-Monette ZY, Abramson J, et al. EBV-positive DLBCL frequently harbors somatic mutations associated with clonal hematopoiesis of indeterminate potential. Blood Advances 2023;7(7):1308–1311. DOI: 10.1182/bloodadvances.2022008550. [PubMed: 36399513]
28. Yap LF, Wong AKC, Paterson IC, Young LS. Functional Implications of Epstein-Barr Virus Lytic Genes in Carcinogenesis. Cancers (Basel) 2022;14(23) (In eng). DOI: 10.3390/cancers14235780.
29. Iqbal J, Wright G, Wang C, et al. Gene expression signatures delineate biological and prognostic subgroups in peripheral T-cell lymphoma. Blood 2014;123(19):2915–2923. DOI: 10.1182/blood-2013-11-536359. [PubMed: 24632715]

30. Melenhorst JJ, Chen GM, Wang M, et al. Decade-long leukaemia remissions with persistence of CD4(+) CAR T cells. Nature 2022;602(7897):503–509. DOI:10.1038/s41586-021-04390-6. [PubMed: 35110735]

31. Chihara D, Dores GM, Flowers CR, Morton LM. The bidirectional increased risk of B-cell lymphoma and T-cell lymphoma. Blood 2021;138(9):785–789. DOI: 10.1182/blood.2020010497. [PubMed: 33822002]

32. Wang J, Su M, Wei N, et al. Chronic active Epstein-Barr virus disease originates from infected hematopoietic stem cells. Blood 2024;143(1):32–41. DOI: 10.1182/blood.2023021074. [PubMed: 37824804]

33. Niroula A, Sekar A, Murakami MA, et al. Distinction of lymphoid and myeloid clonal hematopoiesis. Nature medicine 2021;27(11):1921–1927. DOI: 10.1038/s41591-021-01521-4.

34. Kato S, Hamada M, Okamoto A, et al. EBV+ nodal T/NK-cell lymphoma associated with clonal hematopoiesis and structural variations of the viral genome. Blood Advances 2024. DOI: 10.1182/bloodadvances.2023012019.

35. Prinzing B, Zebley CC, Petersen CT, et al. Deleting DNMT3A in CAR T cells prevents exhaustion and enhances antitumor activity. Science translational medicine 2021;13(620):eabh0272. (In eng). DOI: 10.1126/scitranslmed.abh0272. [PubMed: 34788079]

36. Belizaire R, Wong WJ, Robinette ML, Ebert BL. Clonal haematopoiesis and dysregulation of the immune system. Nature Reviews Immunology 2023;23(9):595–610. DOI: 10.1038/s41577-023-00843-3.

37. Baird JH, Epstein DJ, Tamaresis JS, et al. Immune reconstitution and infectious complications following axicabtagene ciloleucel therapy for large B-cell lymphoma. Blood Adv 2021;5(1):143–155. DOI: 10.1182/bloodadvances.2020002732. [PubMed: 33570626]

38. Hamilton MP, Miklos DB. Chimeric Antigen Receptor T-Cell Therapy in Aggressive B-Cell Lymphoma. Hematol Oncol Clin North Am 2023 (In eng). DOI: 10.1016/j.hoc.2023.05.007.

39. Rejeski K, Perez A, Sesques P, et al. CAR-HEMATOTOX: a model for CAR T-cell-related hematologic toxicity in relapsed/refractory large B-cell lymphoma. Blood 2021;138(24):2499–2513. DOI: 10.1182/blood.2020010543. [PubMed: 34166502]

40. Nair R, Ayers A, Nastoupil LJ, et al. CD19 CAR-T Outcomes in Patients with EBV-Positive DLBCL. Blood 2022;140(Supplement 1):3800–3802. DOI: 10.1182/blood-2022-171120.

41. Jakobsen NA, Turkalj S, Zeng AGX, et al. Selective advantage of mutant stem cells in clonal hematopoiesis occurs by attenuating the deleterious effects of inflammation and aging. bioRxiv 2023:2023.09.12.557322. DOI: 10.1101/2023.09.12.557322.

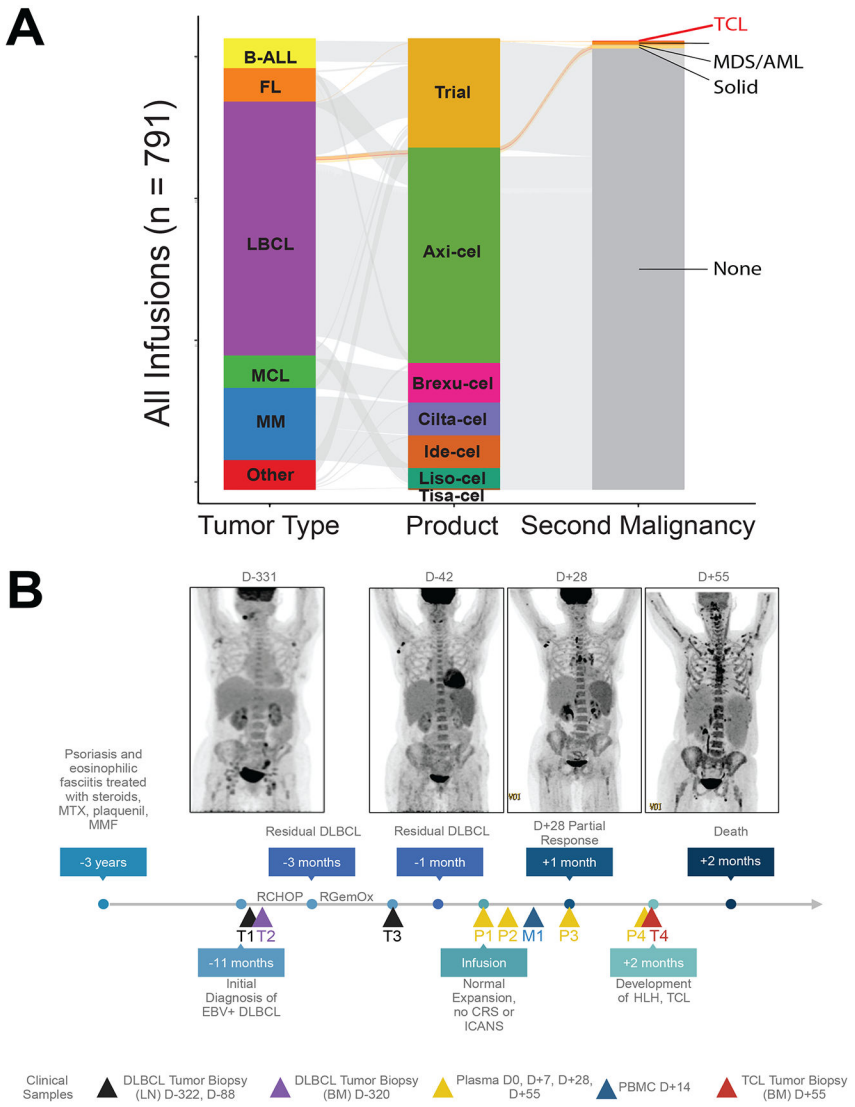

Figure 1: Development of post-CAR19 T-cell lymphoma is rare.

A) Screening 724 patients treated with CAR T-cell therapy at Stanford reveals a single T-cell lymphoma developed after standard of care axi-cel infusion. Experimental products that were eventually approved for commercial distribution are included under the commercial name in this figure for the purpose of clarity. **B)** The index patient was a 59-year-old female with an EBV^{+} DLBCL refractory to RCHOP and RGemOx chemotherapy. She subsequently developed an EBV^{+} PTCL-NOS noted on day 54 leading to hemophagocytic lymphohistiocytosis and death. Axi-cel – axicabtagene autoleucel. Timepoints for major sequencing experiments used in this manuscript are listed in the timeline. DLBCL – Diffuse large B-cell lymphoma, TCL – T-cell lymphoma, RCHOP – Rituximab, cyclophosphamide, hydroxydaunorubicin (Adriamycin), oncovin/vincristine, and prednisone, R-RGemOx – rituximab, gemcitabine, oxaliplatin, CRS – cytokine release syndrome, ICANS – immune effector cell associated neurotoxicity syndrome, MTX – methotrexate, MMF – mycophenolate mofetil, HLH – hemophagocytic lymphohistiocytosis.

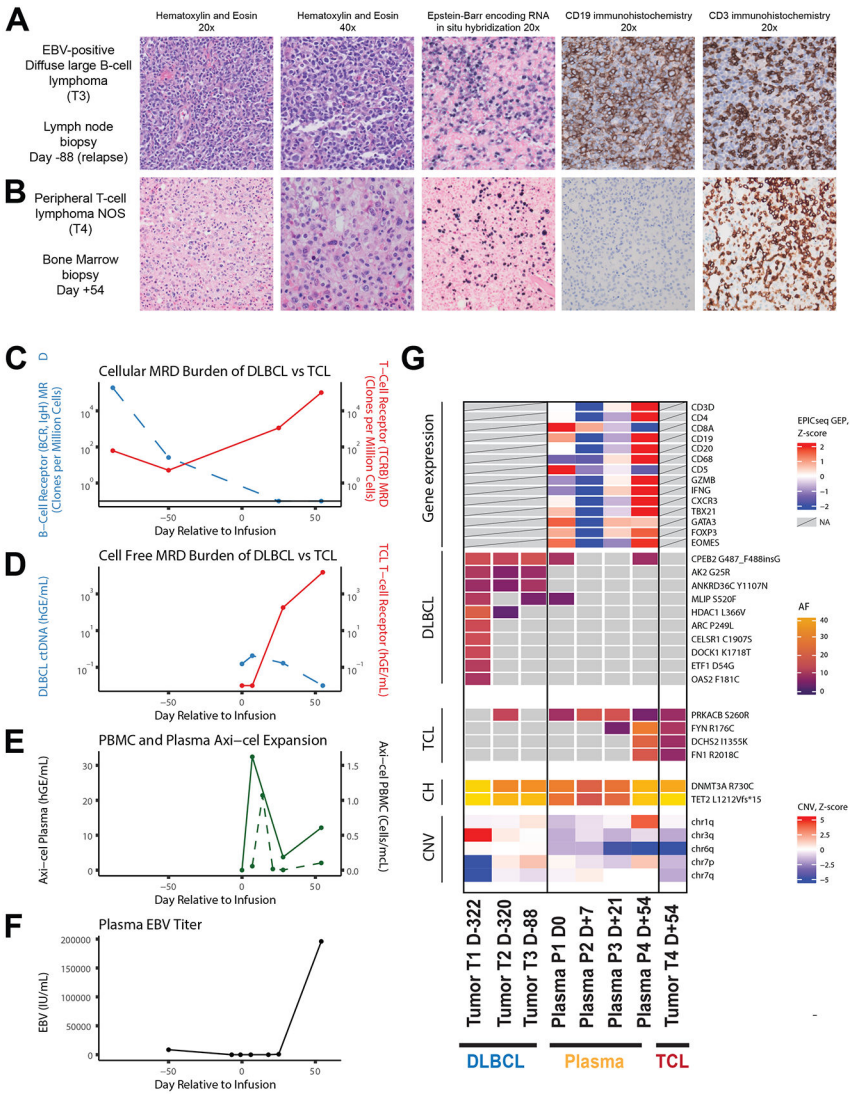

Figure 2: Clinical and molecular characteristics of the index TCL suggest molecular distinction from the DLBCL clone.

A) Immunohistochemistry (IHC) of the original DLBCL tumor in the lymph node demonstrated an abnormal large cell population that was $CD19^{+}CD20^{+}EBER^{+}$. **B)** IHC of the $CD3^{+}CD4^{+}CD8^{-}EBER^{+}$ index T-cell lymphoma **C)** BCR Clonotype analysis; loss of DLBCL BCR detection after axi-cel infusion measured by cellular profiling of the LN, blood and bone marrow (clonoSEQ). Longitudinal data points depicted in order from: 1) DLBCL lymph node at Day −88, 2) peripheral blood at Day −50, 3) peripheral blood at Day 25, 4) Bone marrow harboring TCL. TCRB tracing was performed by identifying the dominant clone in the index bone marrow specimen and determining clonal abundance in prior samples normalized as clones per million nucleated cells (see Methods). **D)** CAPP-Seq profiling of the plasma. There was low-level detection of the original DLBCL at the time of axi-cel infusion which subsequently became undetectable by. At D+28 a novel TCR clone associated with the index TCL was detectable in the plasma by DNA capture profiling. This clone dominated circulation at the time the TCL became clinically apparent. **E)** Axi-

cel expansion and retraction measured by hybridization capture sequencing (CAPP-Seq, solid line) and flow cytometry (dotted line). **F)** Concurrent with development of the index TCL EBV titers rose dramatically in clinical profiling of the plasma. **G)** Comprehensive molecular profiling of longitudinal samples by CAPP-Seq. Panel 1 demonstrates increased malignant TCR clonal load and increased EBV expression in conjunction with gain of CD3 and CD4 expression measured by TSS entropy (EPIC-seq). Grey boxes with diagonal line indicate no data available. Panels 2 and 3 demonstrate the molecular mutational spectrum associated with the original DLBCL and the index TCL are distinct providing no evidence of trans-differentiation of the original B-cell malignancy. Grey boxes indicate the mutation is not detected. Panel 4 demonstrates high burden of pre-existing DNMT3A and TET2 clonal hematopoiesis which was present at the time of diagnosis and remained at high levels throughout the patient's course. Panel 5 demonstrates the presence of copy number variation in the original DLBCL and the index TCL. DLBCL has a distinct chr3q gain whereas the TCL has a distinct chr1q and chr6q loss. BCR – B-cell receptor. CAPP-Seq - CAncer Personalized Profiling by deep Sequencing. TCR – T-cell receptor. EBV – Epstein-Barr virus. TSS – transcription start site. LN – lymph node. BM – bone marrow.

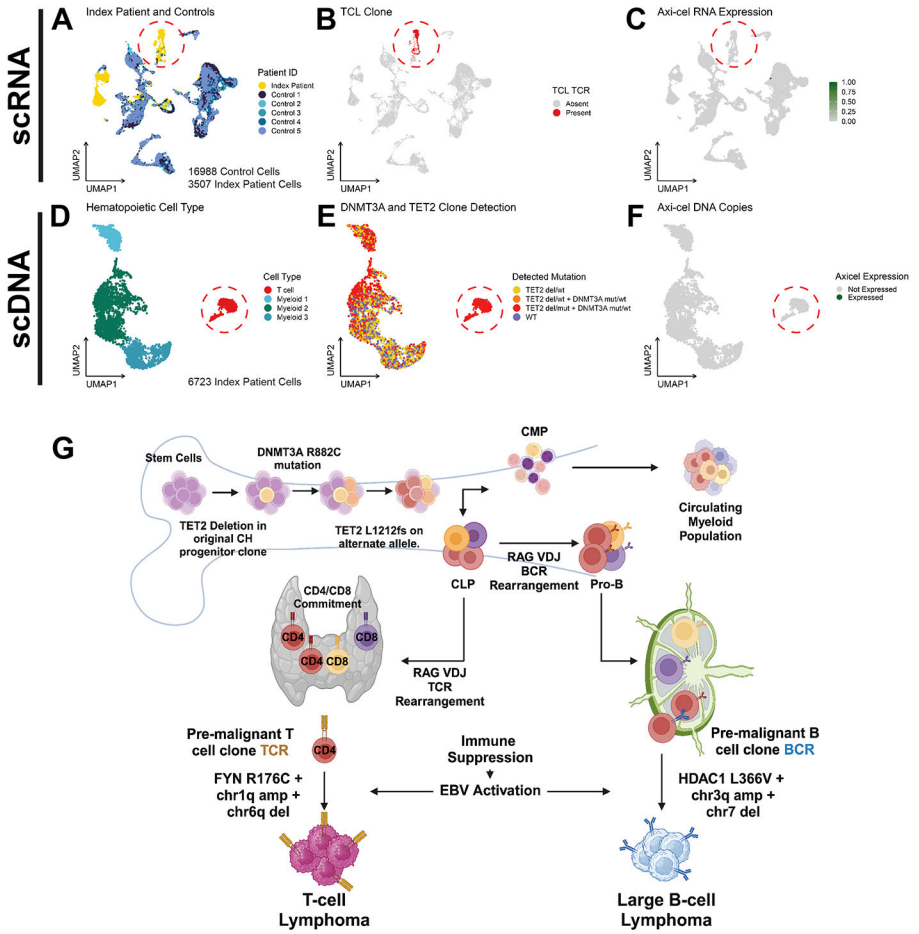

Figure 3. RNA and DNA profiling of the index TCL at single cell resolution shows no evidence of axi-cel vector integration.

A) scRNA analysis of the index patient marrow versus five healthy control marrows demonstrates distinct clustering of the pathologic marrow consistent with the presence of TCL and HLH. **B)** Single cell TCR sequencing reveals the previously described TCL clone found in the plasma matches the T-cell cluster present in the index lesion. **C)** There is complete absence of axi-cel mRNA expression at single cell resolution in the index TCL. **D)** Cell surface antibody profiling combined with single cell DNA profiling again reveals the characteristic $CD3^{+}CD4^{+}CD8^{-}$ malignant clone clustering separately from myeloid cell types. **E)** scDNA profiling of the pre-existing DNMT3A R882C, TET2 deletion, and TET2 L1212Vfs clone. The myeloid populations also have the same clonal hematopoiesis mutations detected. The TET2 L1212Vfs clone is hemizygous following an initiating *TET2* single copy deletion that preceding the *DNMT3A* and *TET2* mutations. Annotations as follows: TET2 del/wt – TET2 deletion only, TET2 del/wt + DNMT3A mut/wt – TET2 deletion + DNMT3A R882C, TET2 del/mut + DNMT3A mut/wt – TET2 deletion + DNMT3A R882C + TET2 L1212Vfs. **F)** scDNA sequencing of axi-cel using an 11-amplicon panel tiled across the axi-cel vector again fails to demonstrate any evidence of axi-cel integration into the index TCL. scRNA – single cell RNA. scDNA – single cell DNA. UMAP – Uniform manifold approximation and projection. Red circles indicate T-cell lymphoma cluster location in each UMAP plot. **G)** Schematic of parallel development of

LBCL and TCL from a common hematopoietic progenitor cell population. Single cell DNA sequencing data indicates a linear accumulation of clonal hematopoiesis (*TET2* deletion → DNMT3A R882C mutation → TET2 L1212fs mutation). The presence of this mutation in all cell populations in scDNA sequencing data indicates the founder population was in hematopoietic stem cells which propagated into the common lymphoid progenitor and common myeloid progenitor (CLP and CMP). Both the DLBCL and TCL tumors contain recombined BCR and TCR respectively consistent with mature lymphoid neoplasms and indicating the DLBCL was derived after germinal center maturation and the TCL was post-thymic. EBV-activation due to immune suppression were likely common events in both tumors but led to unique subsequent mutation and structural variation that resulted in the mature neoplasm. The malignant clones can be traced both by their respective BCR and TCR sequences as well as their unique mutational and structural changes. TCR – T-cell receptor, BCR – B-cell Receptor, BM – bone marrow, CH – clonal hematopoiesis.